

Frame Time-Hopping Fiber-Optic Code-Division Multiple Access Using Generalized Optical Orthogonal Codes

Amir R. Forouzan, Jawad A. Salehi, *Member, IEEE*, and Masoumeh Nasiri-Kenari, *Member, IEEE*

Abstract—In this paper, a new spreading technique for intensity modulation direct detection fiber-optic code-division multiple-access (FO-CDMA) communication systems is proposed. This new spreading technique is based on generalized optical orthogonal codes (OOC) with large cardinality and minimal degradation in performance when compared with a more optimum system, namely, an optical CDMA system using OOC with autocorrelation and cross-correlation value bounded by one, i.e., OOC ($\lambda = 1$). To obtain the performance of such systems, we use a recently introduced communication scheme, namely, frame time-hopping (FTH)-CDMA with random coding. It is discussed that systems with generalized OOC patterns and random time-hopping coding are close in structure and performance. Furthermore, the performance of such systems is near the performance of optical CDMA with optimum but low cardinality OOC ($\lambda = 1$), which further renders the practicality of the proposed technique with very large cardinality. Two new receiver structures for FO-CDMA, namely, chip-level detector with optimum comparator threshold and correlation receiver with an electrical hard limiter, are also proposed. Performance analysis for a binary pulse position FTH-FO-CDMA network is considered for the correlation receiver, chip-level detector, correlation receiver with an optical hard limiter, optimum receiver, and the two newly proposed receiver structures. The results also show that a chip-level detector with optimum comparator threshold is superior to a chip-level detector for received low signal powers, and predict that the performance of the correlation receiver with an electrical hard limiter is superior to all other considered receiver structures, e.g., requiring one third of transmission power to achieve a desired bit error rate when compared with other receiver structures.

Index Terms—Chip-level detector, frame time-hopping (FTH), optical code-division multiple access (CDMA), optical hard limiter, optical orthogonal codes (OOC).

I. INTRODUCTION

OPTICAL code-division multiple access (CDMA) schemes based on intensity modulation/direct detection (IM/DD) not only utilize the potential of fiber-optic capacity but also remain compatible with today's widely used IM/DD optical communications systems. Among the very early techniques that

were introduced for IM/DD optical CDMA employed unipolar optical orthogonal codes (OOCs) with autocorrelation (λ_a) and cross-correlation (λ_c) value bounded by one [1], [2]. Though these classes of OOCs ($\lambda_a = \lambda_c = \lambda = 1$) remain optimum from a multiaccess interference point of view, they suffer from low cardinality, which was shown to be on the order of

$$N(\lambda = 1) \leq \frac{F - 1}{w(w - 1)} \quad (1)$$

where N is the number of OOCs, F the code length, and w the weight of the code. To improve upon the cardinality of the proposed OOCs, one must increase or relax the stringent requirement on the autocorrelation and cross-correlation value. Therefore, a tradeoff exists between the number of codes (users) and the error performance due to increased multiaccess interference. In this paper, our goal is to study and analyze the performance of less structured OOC codes that allow a large increase in the number of users without a large loss in its performance. In [3], the authors considered OOC codes with autocorrelation and cross-correlation value bounded by two. The cardinality of this code is

$$N(\lambda = 2) \leq \frac{(F - 1)(F - 2)}{w(w - 1)(w - 2)} \quad (2)$$

which is considerably higher than OOC with $\lambda = 1$. For typical values of $F = 2000$ and $w = 9$ [4], we can have, at most, 27 codewords with $\lambda = 1$ and 7924 codewords with $\lambda = 2$. Despite the complexity in analyzing the performance of the $\lambda = 2$ system in [3], it was shown that the degradation in performance for $\lambda = 2$ OOC codes is not severe, and, in fact, under certain conditions such as for fixed number of users N and code length F , one can increase the weight of the $\lambda = 2$ OOC codes such that it will surpass in performance when compared with $\lambda = 1$ OOC optical CDMA systems. This leads us to believe that further relaxation on the cross correlation may not necessarily severely degrade the performance of an optical CDMA system while increasing dramatically the cardinality of the OOC codes. In [5], a general upper bound on the number of OOC codes was obtained, and it was shown to be

$$N(\lambda) \leq \frac{(F - 1)(F - 2) \cdots (F - \lambda)}{w(w - 1) \cdots (w - \lambda)}. \quad (3)$$

To generalize our scheme, we will consider $\lambda = w - 1$, which implies that we consider all possible codes of length F and weight w (except the corresponding cyclic shifts) regardless

Paper approved by I. Andonovic, the Editor for Optical Networks and Devices of the IEEE Communications Society. Manuscript received October 25, 2001; revised January 15, 2002. This work was supported in part by the Iran Telecom Research Center (ITRC) under Contract 8031471.

A. R. Forouzan is with the Department of Electrical and Computer Engineering, Faculty of Engineering, University of Tehran, Tehran, Iran (e-mail: forouzan@ece.ut.ac.ir).

J. A. Salehi and M. Nasiri-Kenari are with the Electrical Engineering Department, Sharif University of Technology, Tehran, Iran (e-mail: jasalehi@sharif.edu; mnasiri@sharif.edu).

Digital Object Identifier 10.1109/TCOMM.2002.806495

of their mutual cross-correlation value. For sufficiently large values of F and $\lambda = w - 1$, the number of generalized OOC codes is approximately equal to

$$N(\lambda = w - 1) \approx F^{w-1}/w! \geq F^{w-1}/w^w \quad (4)$$

which could be extremely large for typical values of F and w . However, it remains to be seen that the performance of such optical CDMA systems is not severely degraded. But, unfortunately, the methodologies presented in [2] and [3] do not easily lend themselves to obtaining the performance of the generalized OOC optical CDMA systems. In Section II, we will discuss the expression in (4) being similar to that of generating random codes. And, further, taking advantage of a recently introduced frame time-hopping (FTH) scheme with random codes for ultrawideband pulsed radio communications [6], [7], and analytical tools developed to obtain its performance [8], we evaluate the performance of the proposed FTH fiber-optic CDMA (FO-CDMA) using generalized OOC codes.

FTH FO-CDMA using random codes are not optimum in the sense of multiple-access interference reduction like OOCs ($\lambda = 1$), however, we will show that little will be lost in the multiple-access performance of an intensity-modulated FO-CDMA network if we use these patterns instead of OOCs ($\lambda = 1$). Moreover, we show that the multiple-access interference variance of these patterns is equal to OOCs with $\lambda = 1$. Since FTH patterns considered here use random codes, we may deduce that the multiple-access performance of an intensity-modulated FO-CDMA network is not deeply related to the multiple-access properties of the spreading code, but to the code length (processing gain) and the receiver structure.

In this paper, we further suggest two novel receivers by modifying existing receivers. The first is a chip-level detector with an optimum comparator threshold, and the second is a correlation receiver with an electrical hard limiter. We present the performance analysis of the above two receivers in addition to some basic receivers, namely, correlation receiver, correlation receiver with an optical hard limiter, chip-level detector, and optimum receiver employing binary pulse position modulation (BPPM) in the context of an FTH-FO-CDMA network, and compare their performance. The results show that the chip-level detector with optimum comparator threshold achieves lower bit error rates (BERs) when compared to the ordinary chip-level detector suggested in [9] for weak signal powers, while maintaining the desired features of an ordinary chip-level detector for higher received signal powers. The results also show that the correlation receiver with an electrical hard limiter reaches asymptotically close to the optimum receiver for weak signal powers when compared to a chip-level detector and correlation receiver with an optical hard limiter.

The rest of this paper is organized as follows. In Section II, we describe the proposed transmission method in FO-CDMA network, i.e., frame time-hopping spreading format and BPPM data modulation. Section II also presents the structure of some basic receivers and our two novel proposed receivers. We will derive the structure for the optimum receiver in this section. The performance analysis of the receivers is presented in Section III.

Section IV provides some numerical results, and finally, we will conclude this paper in Section V.

II. SYSTEM DESCRIPTION

The FTH FO-CDMA transmission method introduced here is an extension of a previously proposed method in ultrawidebandwidth radio communication schemes [6], [7], which has many similarities to a previously proposed FO-CDMA using OOCs. In both methods, the bit duration (T_b) time is divided into F chip times, and pulse transmission occurs only in w chip time (called marked chips) out of these F chip time positions. w is called the weight of the code and is usually much less than F , the number of chips in a bit. In FO-CDMA using OOCs, the location of the pulses are determined by a user-dedicated OOC codeword or signature sequence, in which the pulses are not necessarily dispersed uniformly in the bit time duration. However, in an FTH format, the w pulses are located apart in sequential frames, each with duration $T_f = T_b/w$. In this system, a user-dedicated pseudorandom sequence is used in order to synchronize transmitter–receiver pairs, and to locate the chip time pulse in each frame indicating the user’s signature sequence. This pseudorandom sequence could be selected for each user independently and could be changed whenever it is needed without any concordance with other users.

A typical transmitted signal power of user k in an FTH FO communication system can be written as

$$p_{\text{tr}}^{(k)}(t) = \sum_{j=-\infty}^{+\infty} p_{T_w} \left(t - jT_f - c_j^{(k)}T_c - d_j^{(k)}T_c/2 \right) \quad (5)$$

where the index j indicates the frame number, $p_{T_w}(\cdot)$ is the transmitted pulse with duration T_w ($T_w \leq T_c/2$), and $\{c_j^{(k)}\}$ is the dedicated pseudorandom sequence for the user k with integer components. The integer number can take on any value between 0 and $N_h - 1$. In the above equation, we have $N_h T_c \leq T_f$, which guarantees the transmission of exactly one pulse in each frame. The pseudorandom sequence is periodic with period N_p , i.e., $c_{j+N_p}^{(k)} = c_j^{(k)}$. $\{d_j^{(k)}\}$ is the binary sequence of the transmitted symbols corresponding to user k . This sequence is w repetitions of the transmitted data sequence, i.e., if the transmitted binary data sequence is $\{D_i^{(k)}\}$, then we have $d_j^{(k)} = D_i^{(k)}$ for $iw \leq j < (i+1)w$.

According to the above definition, an upper bound on the number of codewords of an FTH pattern can be calculated. As we mentioned earlier, the marked position in each frame is selected based on a pseudorandom sequence with independent integer elements between 0 and $N_h - 1$ ($N_h = F/w$). This sequence is periodic with period N_p , which usually equals w . In this case, the number of different codewords is $(N_h)^w = (F/w)^w$. For transmitter–receiver synchronization, the circular shifts of the codewords is usually eliminated. Since a circular shift of an FTH pattern is not necessarily a valid FTH pattern, this elimination reduces the number of codewords by a factor of, at most, F . Thus, a lower bound on the number of codewords of an FTH code with length F and weight w is

$$N_{\text{FTH}} \geq F^{w-1}/w^w. \quad (6)$$

The above number is considerably larger than the upper bound on the number of OOC codewords with autocorrelation and cross correlation bounded by one [(1)], but it is in the same order of the bound in (4) for generalized OOCs, thus, highlighting the close similarities that exist between these two coding schemes.

The signals are transmitted through an $N \times N$ optical star coupler to the receivers. We assume a lossless star coupler that ideally divides the received power in all of its incoming branches at its outgoing branches equally. In this case, the expected value of the received power from user k at the output of the desired receiver (receiver 1) photodetector can be written as

$$\begin{aligned} \bar{p}_{\text{rec}}^{(k)}(t) &\triangleq E \left\{ p_{\text{rec}}^{(k)}(t) \right\} = \frac{1}{N} p_{\text{tr}}^{(k)}(t - \tau_k) \\ &= \frac{1}{N} \sum_{j=-\infty}^{+\infty} p_{T_w} \left(t - jT_f - c_j^{(k)}T_c - d_j^{(k)}T_c/2 - \tau_k \right) \end{aligned} \quad (7)$$

where τ_k is the delay of user k , and $1/N$ is the attenuation factor of the $N \times N$ optical star coupler. We assume that each received pulse produces a photoelectron count with mean m_r at the output of the photodetector. As can be seen, the FO dispersion effect is not considered in the above equation, and it is considered that the transmitted pulses are received with the same duration as they were transmitted. However, if the dispersion effect were such that the received pulse duration is not more than $T_c/2$, the following performance analysis is still valid.

Without loss of generality, we assume that τ_1 is zero and $0 \leq \tau_k < T_f$ for all $2 \leq k \leq N$, and we further assume a chip-synchronous network and uniform distributed time delays τ_k 's, which results in an upper bound on the performance of the system [1].

Receiver Structures

The receiver utilizes a photodetector with quantum efficiency η , and it is synchronous with the desired user (user 1), i.e., the receiver knows the desired signal delay, τ_1 , and the corresponding pseudorandom sequence for user 1, $\{c_j^{(1)}\}$. In the following, we discuss the structure of the most viable receivers for incoherent FO-CDMA systems for FTH-FO-CDMA. Moreover, two novel receivers, namely, a chip-level detector with optimum comparator threshold and correlation receiver with an electrical hard limiter, will be introduced.

Since our objective is to study FTH-FO-CDMA system capabilities and drawbacks, we have selected a straightforward realization of the considered receivers. However, most of these receivers could be realized in other forms, especially in an all-optical structure.

A. Correlation Receiver

In this receiver and for the BPPM data modulation format, the received photoelectrons in the first slots of the w marked chips in a bit duration are added together, and then compared to the sum of the received photoelectrons in the second slots of

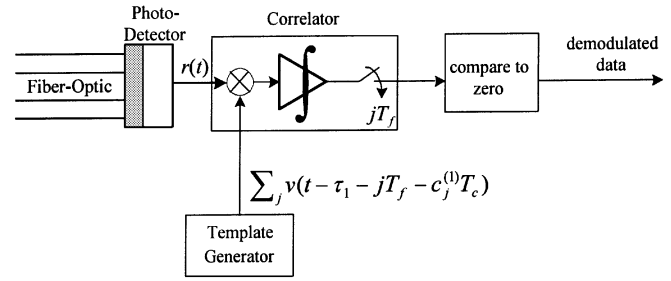


Fig. 1. Typical correlation receiver [see (9)].

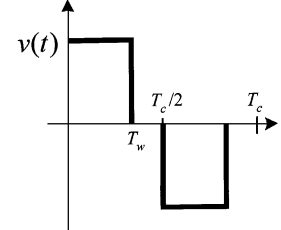


Fig. 2. Receiver's template signal.

the marked chips to detect the transmitted data bit. Thus, the receiver decides based on the following decision rule:

$$\begin{aligned} \text{"decide that } D_0^{(1)} = 0\text{"} &\Leftrightarrow \\ &\int_{\tau_1}^{\tau_1 + wT_f} r(t) \sum_{j=0}^{w-1} p_{T_w} \left(t - \tau_1 - jT_f - c_j^{(1)}T_c \right) dt \\ &> \int_{\tau_1}^{\tau_1 + wT_f} r(t) \sum_{j=0}^{w-1} p_{T_w} \left(t - \tau_1 - jT_f - c_j^{(1)}T_c - T_c/2 \right) dt \end{aligned} \quad (8)$$

where $D_0^{(1)}$ is the desired user (user 1) data bit. This decision rule can be reduced to the following equation [7] (Fig. 1):

$$\begin{aligned} \text{"decide that } D_0^{(1)} = 0\text{"} &\Leftrightarrow \\ &\underbrace{\sum_{j=0}^{w-1} \int_{\tau_1 + jT_f}^{\tau_1 + (j+1)T_f} r(t)v \left(t - \tau_1 - jT_f - c_j^{(1)}T_c \right) dt}_{\text{test statistic}} > 0 \end{aligned} \quad (9)$$

where $v(t) \triangleq p_{T_w}(t) - p_{T_w}(t - T_c/2)$ is the receiver's template signal (Fig. 2).

B. Correlation Receiver With an Optical Hard Limiter

Salehi and Brackett [2] have suggested placing an optical hard limiter before the photodetector of a correlation receiver. This device limits the multiuser interference and improves the receiver performance (Fig. 3). An ideal optical hard limiter is defined as [2]

$$g(x) = \begin{cases} Q, & \text{if } x \geq Q \\ 0, & \text{otherwise} \end{cases} \quad (10)$$

where x is the received optical light intensity and Q is the device threshold usually considered to be the same as the mean of the desired user pulse intensity.

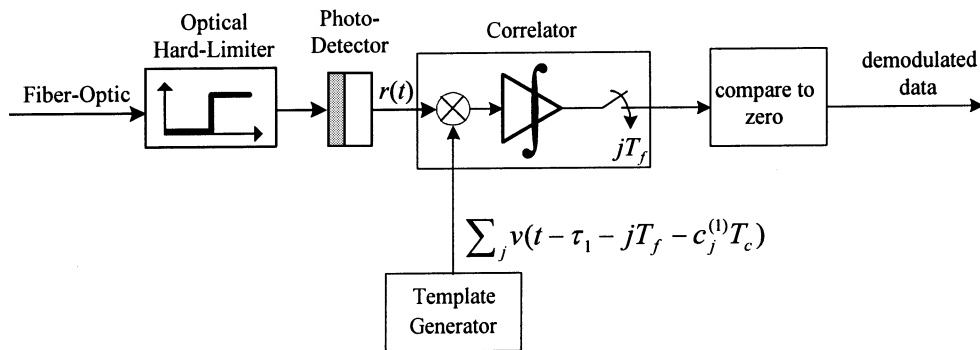


Fig. 3. Correlation receiver with an optical hard limiter.

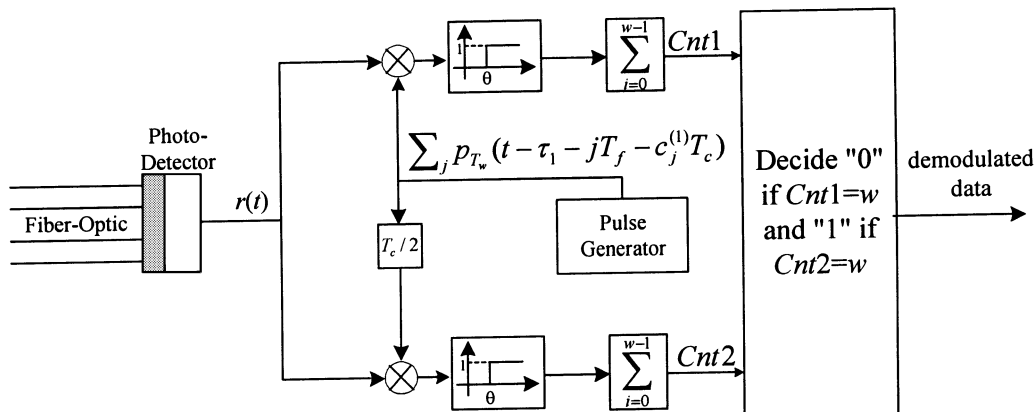


Fig. 4. Chip-level detector.

C. Chip-Level Detector

A chip-level detector [9] (Fig. 4) uses a thresholder after the photodetector to detect the received signal in the first and the second slots of each marked chip separately. If the signal is present in all of the w first slots of the marked chips, it detects a "0." On the other hand, if the signal is present in all of the second slots of the marked chips, it detects a "1." If both or none of the above conditions is true, the receiver decides randomly and with equal probability a "0" or a "1." Suppose that $Cnt1$ counts the number of marked chips that the received photoelectrons in their first slots is equal to or more than the threshold value θ , and $Cnt2$ counts the number of marked chips that the received photoelectrons in their second slots is equal to or more than the threshold value θ . With the above definitions, the decision rule for a chip-level detector can be written as

$$\text{Decide} \begin{cases} D_0^{(1)} = 0, & \text{if } Cnt1 = w \text{ and } Cnt2 < w \\ D_0^{(1)} = 1, & \text{if } Cnt2 = w \text{ and } Cnt1 < w \\ \text{randomly}(0, 1), & \text{otherwise.} \end{cases} \quad (11)$$

Considering an ideal photodetector, it was shown that this receiver is optimum in the case of deterministic codes and nearly all cases of random codes [10].

D. Chip-Level Detector With Optimum Comparator Threshold

Suppose the desired user has sent a "0." That is, it has sent pulses in the first slots of the w marked chips and it has not sent any pulses in the second slots of these chips. When the noise is weak, the probability of detecting signals in all of the second slots of these w chips is small, but due to the shot-noise effect of the photodetector, it is possible not to receive the signal in the first slot of at least one marked chip, which will result in a detection error with probability $1/2$ [see (11)]. In this case, if we change the decision rule in (11) to the following rule, we get a receiver with a better performance (Fig. 5)

$$\text{Decide} \begin{cases} D_0^{(1)} = 0, & \text{if } Cnt1 \geq w' \text{ and } Cnt2 < w' \\ D_0^{(1)} = 1, & \text{if } Cnt2 \geq w' \text{ and } Cnt1 < w' \\ \text{randomly}(0, 1), & \text{otherwise} \end{cases} \quad (12)$$

where w' is an integer less than or equal to w and is called the comparator threshold. In this paper, we assume that the receiver can change the comparator threshold adaptively to achieve the best performance (minimum probability of bit error). The bit error probability of this receiver is a lower bound for any receiver with a deterministic comparator threshold. However, this receiver is more complicated because it requires

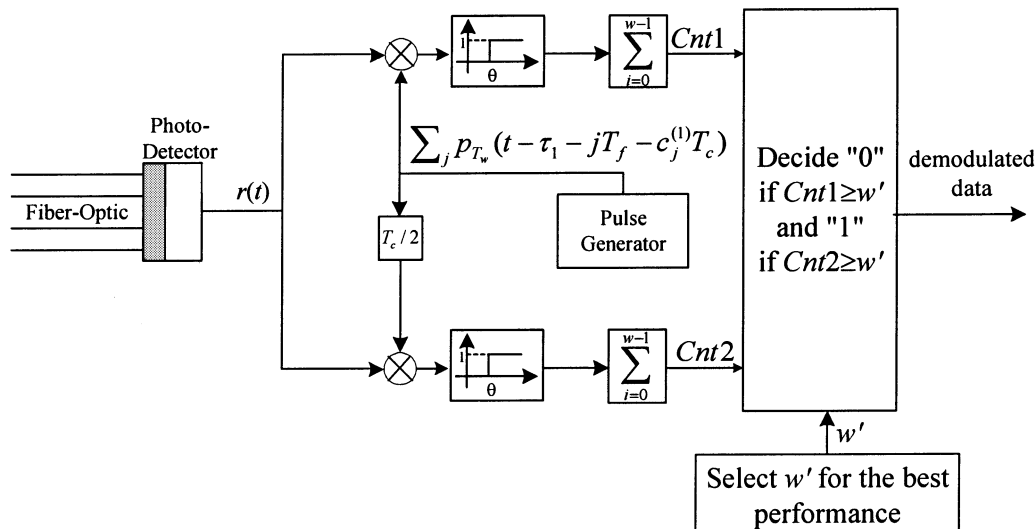


Fig. 5. Chip-level detector with optimum comparator threshold.

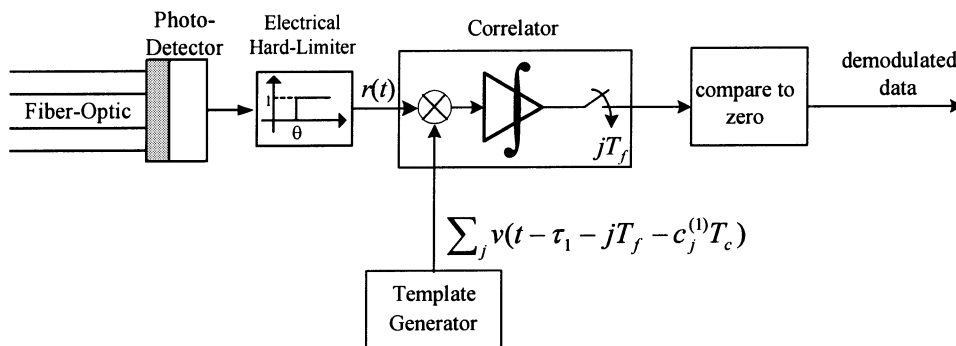


Fig. 6. Correlation receiver with an electrical hard limiter.

the knowledge of the network conditions to adaptively choose the best threshold.

E. Correlation Receiver With an Electrical Hard Limiter

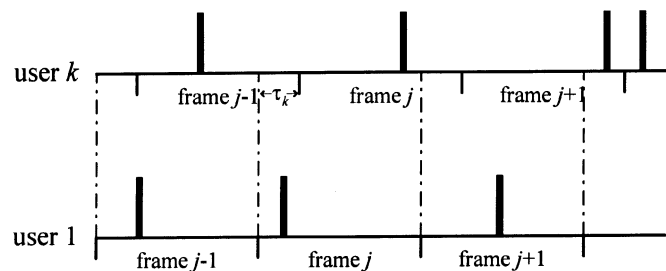
Changing the above decision rule (12) to (13), we achieve a simpler receiver with a better performance

$$\text{Decide } \begin{cases} D_0^{(1)} = 0, & \text{if } \text{Cnt1} > \text{Cnt2} \\ D_0^{(1)} = 1, & \text{if } \text{Cnt1} < \text{Cnt2} \\ \text{randomly}(0, 1), & \text{otherwise} \end{cases} \quad (13)$$

i.e., the receiver detects the data by comparing the counters. One can simply show that this receiver is equal to a correlation receiver that uses an electrical hard limiter after the photodetector (Fig. 6). This receiver does not require selecting a threshold, so it is simpler than the chip-level detector with optimum comparator threshold. Furthermore, we see that the first and the second conditions in (12) result in the first and the second conditions of (13), respectively. Thus, the BER of this detector is a lower bound for the BER of a chip-level detector with optimum comparator threshold.

F. Optimum Receiver

In this section, we first develop some basic mathematical tools that are used first, in the derivation of the optimum receiver


 Fig. 7. Received pulse streams of user 1 and user k .

structure, and second, in the performance analysis of some other receiver structures. Consider an arbitrary interfering user k ($k \neq 1$). First, we study the interference of this user in just one frame. As we discussed previously, in an FTH format, the pulses are nearly uniformly spread over the bit time, and there are w frames and w pulses in a bit duration for any user. Consider the marked chip in an arbitrary frame j of user 1. This marked chip could be occupied by the j th or $j - 1$ th pulse of user k . As can be seen from Fig. 7, if the marked chip of the j th frame of user 1 is located before the beginning of the j th frame of user k , it is possible to be interfered with by the $j - 1$ th pulse of user k , otherwise it could be interfered with by the j th pulse of user k . In either case, since there exist $2N_h = 2F/w$ possible locations for any pulse of user k and two slots in any marked chip,

the probability that the interfering pulse of user k hits the j th marked chip of user 1 is $\beta = 2/(2N_h) = w/F$. Thus, the probability of a hit in the first slot of a marked chip of user 1 is equal to the probability of a hit in its second slot, and is $\beta/2 = 1/(2N_h) = w/(2F)$. The probability of no interference is $\alpha = 1 - \beta = 1 - w/F$.

Using the above explanation, we obtain the decision rule for the optimum receiver in Appendix A as follows:

$$\prod_{i=1}^w s_i \stackrel{0}{\leq} \prod_{i=1}^w t_i \quad (14)$$

where s_i and t_i , $1 \leq i \leq w$, are the number of pulses received in the first and second slots of the i th marked chip, respectively. The decision rule (14) is the same as the optimum decision rule for the OOC with $\lambda = 1$, obtained in [9].

III. PERFORMANCE EVALUATION

In this section, we present multiple-access performance analysis of the FTH format for the above six receiver structures. We assume a chip-synchronous network, and since our main objective is to compare the multiple-access performance of the FTH method with the OOC method, we neglect background noise, circuit thermal noise, and photodetector dark current, since their influences on the system performance are the same for both methods. However, the photodetector shot noise is considered for all receivers except the optimum receiver, which is derived only for the ideal photodetector case.

A. Correlation Receiver

To facilitate the performance evaluation, we employ a saddle-point approximation technique [11] which basically relies on the probability characteristic function of the output correlator. Assume user 1 has sent a "0." With w pulses in a bit, each with mean photoelectron count m_r , at the output of photodetector, the desired user signal has a Poisson distribution with mean $w m_r$ at the output of the correlator. Thus, the characteristic function of the desired signal is

$$\Phi_s(z) = \exp(-w m_r(1 - z)). \quad (15)$$

We denote by $\alpha_j^{(k)}$ the interference of a single interfering user $k \neq 1$ in frame j at the output of the correlator. It can be shown that the probability function of $\alpha_j^{(k)}$ is

$$p_{\alpha_j^{(k)}}(n) = \frac{\beta}{2} [Pos(m_r, n) + Pos(m_r, -n)] + \alpha \delta(n) \quad (16)$$

where $\alpha = 1 - w/F$, $\beta = w/F$, and $\delta(\cdot)$ is Dirac's impulse function. The probability characteristic function of $\alpha_j^{(k)}$ is

$$\Phi_{\alpha_j^{(k)}}(z) = \alpha + \frac{\beta}{2} [\exp(-m_r(1 - z)) + \exp(-m_r(1 - z^{-1}))]. \quad (17)$$

The total multiple-access interference in a bit duration is the sum of the interference due to all other users k for $2 \leq k \leq N$ on all

frames j , $1 \leq j \leq w$, of a bit. We assume that the interference is independent in different frames of a bit. Thus, the probability characteristic function of the interference in a bit duration is

$$\Phi_{MA}(z) = \left[\alpha + \frac{\beta}{2} [\exp(-m_r(1 - z)) + \exp(-m_r(1 - z^{-1}))] \right]^{w(N-1)} \quad (18)$$

where N is the number of active users. Multiplying (15) by (18), we get the probability characteristic function of the output of the correlator conditioned on the input bit being binary data "0"

$$\Phi(z) = \exp(-w m_r(1 - z)) \left[\alpha + \frac{\beta}{2} [\exp(-m_r(1 - z)) + \exp(-m_r(1 - z^{-1}))] \right]^{w(N-1)}. \quad (19)$$

Using saddle-point approximation [11], we obtain the BER of a correlation receiver from the above equation. We have $P_E = (1/2)P_{E|0} + (1/2)P_{E|1}$, but for BPPM $P_{E|0} = P_{E|1}$, then

$$\begin{aligned} P_E &= P_{E|0} \\ &= \Pr\{\text{Correlator output being less than Th} | 0\} \\ &\approx \frac{\exp[\Psi(s_1)]}{\sqrt{2\pi\Psi''(s_1)}} \end{aligned} \quad (20)$$

where $\Psi(s) = \ln(\Phi(e^s)e^{-\text{Th}\cdot s}/|s|)$, $\Psi''(s) \triangleq d^2\Psi(s)/ds^2$, s_1 is the negative root of equation $\Psi'(s) = d\Psi(s)/ds = 0$, and Th is the decision comparator threshold, which is zero in our application [see (9)].

B. Correlation Receiver With an Optical Hard Limiter

Once again, we assume that the transmitted data bit is zero and we assume that the optical hard-limiter threshold (Q) is equal to the intensity of the desired user-received pulse, that is, the least required level for detecting data and in order to reject the interference as much as possible. Assuming the data bit is zero and also considering the optical hard-limiter effect, which removes interference from the first slots of the marked chips, a Poisson photoelectron count with mean m_r at the output of the photodetector in the first slot of the marked chips will be detected. The sum of these signals will be a Poisson photoelectron count with mean $w m_r$ at the output of the correlator. However, an optical hard limiter cannot block the received interference in the second slots of the marked chips, but limits its intensity to the intensity of just one chip pulse. Since there exist $N - 1$ interfering users, and each may send a signal in the second slot of a marked chip independently with probability $\beta/2 = w/(2F)$, the probability of detecting a signal in the second slot of this marked chip is $p_c = 1 - (1 - \beta/2)^{N-1}$.

We assume that the interference is independent in different frames of a bit. Thus, the probability of detecting a signal in ℓ slots out of w second slots of the marked chips is $\binom{w}{\ell} p_c^\ell (1 - p_c)^{w-\ell}$, which will result in a negative Poisson photoelectron

count with mean ℓm_r at the output of the correlator. Consequently, the probability of error is

$$\begin{aligned}
P_E &= P_{E|0} \\
&= \sum_{\ell} \Pr\{\text{Signal detection in } \ell \text{ second slots} \\
&\quad \text{of the marked chips} | 0\} \\
&\quad \times \left(\Pr\{X_{w m_r} < X_{\ell m_r}\} + \frac{1}{2} \Pr\{X_{w m_r} = X_{\ell m_r}\} \right) \\
&= \sum_{\ell=0}^w \binom{w}{\ell} p_c^\ell (1-p_c)^{w-\ell} \\
&\quad \left(\sum_{i=0}^{\infty} \exp(-w m_r) (w m_r)^i / i! \right. \\
&\quad \times \sum_{j=i+1}^{\infty} \exp(-\ell m_r) (\ell m_r)^j / j! \\
&\quad \left. + \frac{1}{2} \sum_{i=0}^{\infty} \exp(-(w+\ell) m_r) (w \ell m_r^2)^i / (i!)^2 \right) \quad (21)
\end{aligned}$$

where $X_{\bar{m}}$ denotes a Poisson random variable with mean \bar{m} .

C. Chip-Level Detector

1) *Ideal Photodetector*: We assume that the threshold value θ is one. Since the modulation is BPPM, the probability of error is equal to the probability of error conditioned on the transmitted data bit being binary “zero.” In an ideal case, when the transmitter sends a binary data “zero,” the energy will be detected in all of the first slots of the marked chips in the receiver. Thus, the error in detection is only possible when the detector detects energy in all of the second slots of the marked chips, also. Since there are w marked chips, the probability of error is

$$P_E = \frac{1}{2} (p_c)^w = \frac{1}{2} [1 - (1 - \beta/2)^{N-1}]^w \quad (22)$$

where the factor $1/2$ stands for the receiver random selection of “zero” and “one” in the case both counters are equal to w [see (11)].

2) *Quantum-Limit Performance*: In this case, the received pulses produce a Poisson photoelectron count with a mean m_r at the output of the photodetector. We assume that the receiver threshold is set to θ . Thus, conditioned on the transmitted data bit being “zero,” the error occurs on the following three cases [(11)].

Case 1) The first counter is less than w and the second counter is equal to w . In this case, the receiver detects a wrong bit with probability 1.

Case 2) Both output counters are equal to w .

Case 3) Both of the counters are less than w . For the latter two cases, the receiver detects a wrong bit with probability $1/2$.

Hence

$$\begin{aligned}
P_E &= \Pr\{\text{Cnt1} < w \text{ and Cnt2} = w | 0\} \\
&\quad + \frac{1}{2} \Pr\{\text{Cnt1} = w \text{ and Cnt2} = w | 0\}
\end{aligned}$$

$$\begin{aligned}
&\quad + \frac{1}{2} \Pr\{\text{Cnt1} < w \text{ and Cnt2} < w | 0\} \\
&= \frac{1}{2} (\Pr\{\text{Cnt1} < w \text{ and Cnt2} = w | 0\} \\
&\quad + \Pr\{\text{Cnt1} = w \text{ and Cnt2} = w | 0\}) \\
&\quad + \frac{1}{2} (\Pr\{\text{Cnt1} < w \text{ and Cnt2} = w | 0\} \\
&\quad + \Pr\{\text{Cnt1} < w \text{ and Cnt2} < w | 0\}). \quad (23)
\end{aligned}$$

Since the counters are always less than or equal to w , we have

$$P_E = \frac{1}{2} \Pr\{\text{Cnt2} = w | 0\} + \frac{1}{2} \Pr\{\text{Cnt1} < w | 0\}. \quad (24)$$

The probability of the second counter being w is equal to the probability of the received photoelectron count in the second slot of all w marked chips being greater than or equal to θ . The probability of a hit in the second slot of a marked chip by an interfering user is $\beta/2$, which results in a Poisson photoelectron count with mean m_r ; otherwise, there is no interference in the second slot of this chip. Since there exist $N - 1$ independent interfering users, the probability characteristic function of the total interference in the second slot of a marked chip is

$$\Phi_j^{\alpha_j^1}(z) = \Phi_{MA}^{\alpha_j^1}(z) = \left[1 - \frac{\beta}{2} + \frac{\beta}{2} \exp(-m_r(1-z)) \right]^{N-1}. \quad (25)$$

We denote by p_θ the probability of interference on this slot being greater than or equal to θ that can be evaluated by saddle-point approximations and (25). Since there are w frames in a bit, the probability of the second counter being w is $(p_\theta)^w$.

For calculating the second part of (24), we note that $\Pr\{\text{Cnt1} < w | 0\} = 1 - \Pr\{\text{Cnt1} = w | 0\}$. Using the above methodology, we can similarly calculate the probability of the first counter being w . The only exception is the probability characteristic function of the signal, which contains the desired signal part. Thus, the probability characteristic function of the received photoelectron count in the first slot of a marked chip conditioned on the transmitted data bit of the desired user being “zero” is

$$\begin{aligned}
\Phi_j^{\alpha_j^0}(z) &= \exp(-m_r(1-z)) \\
&\quad \times \left[1 - \frac{\beta}{2} + \frac{\beta}{2} \exp(-m_r(1-z)) \right]^{N-1}. \quad (26)
\end{aligned}$$

We denote by p'_θ the probability of the received desired signal plus the interference signal on the first slot of a marked chip being greater than or equal to θ that can be evaluated in the same way as p_θ , and similarly, the probability of the first counter being w is $(p'_\theta)^w$. Thus

$$P_E = \frac{1}{2} p_\theta^w + \frac{1}{2} - \frac{1}{2} p_\theta'^w. \quad (27)$$

It is important to note that the receiver performance depends on the value of θ , and for various operating conditions, an optimum value for θ exists that minimizes the BER. However, for the sake of simplicity, it is usually selected to be equal to one.

Quantum-Limit Performance for $\theta = 1$: If we assume that the threshold, θ , is equal to one, we can obtain, explicitly, the

BER expression. Since α_j^0 and α_j^1 are two positive random variables, we have

$$p_\theta = 1 - \Phi^{\alpha_j^1}(z) \Big|_{z=0} = 1 - [1 - \beta/2 + e^{-m_r} \beta/2]^{N-1} \quad (28)$$

and

$$p'_\theta = 1 - \Phi^{\alpha_j^0}(z) \Big|_{z=0} = 1 - e^{-m_r} [1 - \beta/2 + e^{-m_r} \beta/2]^{N-1}. \quad (29)$$

Thus

$$P_E = \frac{1}{2} (1 - [1 - \beta/2 + e^{-m_r} \beta/2]^{N-1})^w + \frac{1}{2} - \frac{1}{2} (1 - e^{-m_r} [1 - \beta/2 + e^{-m_r} \beta/2]^{N-1})^w. \quad (30)$$

D. Chip-Level Detector With Optimum Comparator Threshold

As we mentioned earlier, this receiver has a superior performance over an ordinary chip-level detector when photodetector shot noise is the major source of detection error. In the following, we analyze the quantum-limit performance of this receiver. Similar to (24), it can be shown that

$$P_E(w') = \frac{1}{2} (1 - \Pr\{\text{Cnt1} \geq w' | 0\}) + \frac{1}{2} \Pr\{\text{Cnt2} \geq w' | 0\} \quad (31)$$

where by definition $P_E(w')$ is the probability of bit error of a chip-level detector with comparator threshold w' . We recall that p_θ and p'_θ are the probability of the received photoelectron counts in the second and the first slots of a marked chip being greater than or equal to θ , respectively. Since the interference in different frames (or marked chips) is independent; Cnt1 and Cnt2 are two random variables with binomial distribution. Thus

$$\Pr\{\text{Cnt1} \geq w' | 0\} = \sum_{i=w'}^w \binom{w}{i} p_\theta^i (1 - p_\theta)^{w-i}$$

and

$$\Pr\{\text{Cnt2} \geq w' | 0\} = \sum_{i=w'}^w \binom{w}{i} p'_\theta^i (1 - p'_\theta)^{w-i}. \quad (32)$$

As mentioned earlier, both p_θ and p'_θ depend on the number of active users (N) and the received photoelectron count mean (m_r) and can be numerically obtained by saddle-point approximations and the probability characteristic function of the interference in the first and second slots of a marked chip [(25) and (26)]. If the threshold θ is set to one, these values can be evaluated in explicit formulas [(28) and (29)].

Chip-level detector with optimum comparator threshold selects the comparator threshold to achieve the minimum BER by the knowledge of the instantaneous conditions of the network. Thus

$$P_E = \min_{w'} \{P_E(w')\}. \quad (33)$$

The instantaneous conditions of the network can be estimated by measuring the total multiaccess interference in a bit duration or by some means such as using protocol in higher layers of the network.

E. Correlation Receiver With an Electrical Hard Limiter

We recall that with an ideal photodetector, this receiver is the same as the chip-level detector. In the following, we obtain the multiple-access performance of a correlation receiver with an electrical hard limiter considering the photodetector shot noise.

To calculate the BER of a correlation receiver with an electrical hard limiter, we first focus on the probability characteristics of the output of electrical hard limiter in the marked chip of frame 1. We distinguish three different events based on the signal detection in the first and the second slot of this marked chip.

Event A)

Detecting signal only in the first slot of the marked chip.

Event B)

Detecting signal only in the second slot of the marked chip.

Event C)

Detecting signal in both or none of the slots of the marked chip.

We denote by p_A , p_B , and p_C the probability of occurrence of the above three cases, respectively. Assuming that the transmitted bit of user 1 is "zero," p_A and p_B can be calculated by summation on all of the possible interference patterns as

$$p_A = \sum_{\substack{i, j \geq 0 \\ i+j \leq N-1}} \binom{N-1}{i, j, N-1-i-j} (\beta/2)^{i+j} \alpha^{N-1-i-j} \cdot \Pr\{X_{(i+1)m_r} \geq \theta\} \Pr\{X_{jm_r} < \theta\} \quad (34)$$

$$p_B = \sum_{\substack{i, j \geq 0 \\ i+j \leq N-1}} \binom{N-1}{i, j, N-1-i-j} (\beta/2)^{i+j} \alpha^{N-1-i-j} \cdot \Pr\{X_{(i+1)m_r} < \theta\} \Pr\{X_{jm_r} \geq \theta\}. \quad (35)$$

In the above equations, i and j denote the number of interfering users in the first and the second slots of the marked chip, respectively. $X_{(i+1)m_r}$ is the received photoelectron count in the first slot of a marked chip, considering i interfering users in the first slot and the transmitted bit being "zero," and X_{jm_r} is the received photoelectron count in the second slot of a marked chip, considering j interfering users in the second slot and the transmitted bit being "zero." We recall that $X_{(i+1)m_r}$ and X_{jm_r} are two Poisson random variables with means $(i+1)m_r$ and jm_r , respectively. When $\theta = 1$, we have $\Pr\{X_{(i+1)m_r} \geq 1\} = 1 - \exp(-(i+1)m_r)$, $\Pr\{X_{(i+1)m_r} < 1\} = \exp(-(i+1)m_r)$, $\Pr\{X_{jm_r} \geq 1\} = 1 - \exp(-jm_r)$, and $\Pr\{X_{jm_r} < 1\} = \exp(-jm_r)$. p_C can be calculated simply as $p_C = 1 - p_A - p_B$.

Conditioned on the input bit being "zero," the above events are independent in different frames of a bit and considering the electrical hard limiter is followed by a correlator, error occurs when the number of occurrences of event B is greater than or equal to (with probability 1/2) the number of occurrences of event A in w frames of a bit. Thus, we can write the probability of error as

$$P_E = \sum_{\substack{b > a \geq 0 \\ a+b \leq w}} \binom{w}{a, b, w-a-b} (p_A)^a (p_B)^b (p_C)^{w-a-b} + \frac{1}{2} \sum_{\substack{b=a \geq 0 \\ a+b \leq w}} \binom{w}{a, b, w-a-b} (p_A)^a (p_B)^b (p_C)^{w-a-b}. \quad (36)$$

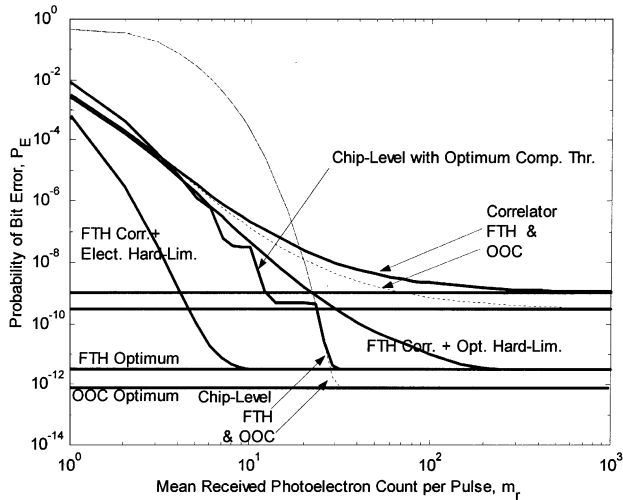


Fig. 8. BER of various receiver structures versus the mean received photoelectron count per pulse for FTH and OOC ($\lambda = 1$) systems with $F = 2000$, $w = 9$, and $N = 27$.

F. Optimum Receiver

In Appendix B, a lower bound on the BER of the optimum receiver is derived as

$$P_E \geq \left[(1 - \beta/2)^{N-1} - (1 - \beta)^{N-1} \right]^w - 2^{-w-1} \left[(N-1)\beta(1 - \beta)^{N-2} \right]^w. \quad (37)$$

IV. NUMERICAL RESULTS

In this section, we evaluate numerically the performance for both FTH (or generalized OOC) and OOC ($\lambda = 1$) transmission methods and discuss the results, such as the BER of various receiver structures versus the number of users and the mean received photoelectron count per pulse.

To plot the performance of OOC ($\lambda = 1$) systems in Fig. 8 and in the subsequent figures, we have used the results in [1]–[5] and [9]. As we mentioned earlier, the maximum number of users in an OOC ($\lambda = 1$) FO-CDMA network is upper bounded by a function of the weight and the length of the OOC ($\lambda = 1$) code, which is not usually a large number. Therefore, in a few figures on BER versus the number of users, we do not include the performance of the OOC ($\lambda = 1$) systems.

We assume the total number of chips in a bit (F) and the code weight (w) to be 2000 and 9, respectively. With this assumption, an upper bound on the number of the OOC ($\lambda = 1$) codewords with autocorrelation and cross correlation (bounded by 1) [(1)] is 27, and the number of the FTH patterns or generalized OOC is more than 6.6×10^{17} [(6)]. As can be seen, the number of codewords in FTH patterns is much larger than the OOC ($\lambda = 1$) codes, i.e., the number of users constraint is completely removed in this method. This fact allows any user to select its codeword without a need to concord with other users, and it is possible to change the codeword in any arbitrary fashion, which could result in a high invulnerability to eavesdropping compared to the OOC ($\lambda = 1$) transmission method.

In Fig. 8, the BER of several receivers is plotted for both FTH patterns and OOC ($\lambda = 1$) codes versus the mean received photoelectron count per pulse (m_r). The number of users in this

figure is 27, which is the maximum number of users that an OOC ($\lambda = 1$) system (with length 2000 and weight 9) could support. Comparing the performance of correlation receiver and chip-level detector for FTH patterns and OOC ($\lambda = 1$) codes, we see that the multiple-access performance of the FTH patterns or generalized OOC is sufficiently close to the best achievable performance by code construction, i.e., employing OOCs with $\lambda = 1$. As can be observed, the multiple-access performance of FTH patterns is, at most, one order of magnitude worse than the OOC ($\lambda = 1$) codes for the correlation, chip-level detector, and optimum (assuming an ideal photodetector) receivers. Especially for the chip-level detector, the performance is the same for the received mean photoelectron counts per pulse less than 30 (the two curves overlap in this region).

This behavior is not strange if we compare the multiple-access interference variance of an OOC ($\lambda = 1$) system by a FTH system. Multiuser interference variance of an FTH system at the output of the correlator can be calculated using (18) as follows:

$$\sigma_{\text{FTH}}^2 = \left. \frac{\partial^2 \Phi_{\text{MA}}(z)}{\partial z^2} \right|_{z=1} = (N-1)w^2 m_r (1 + m_r) / F. \quad (38)$$

For an OOC ($\lambda = 1$) system with the same data modulation (BPPM), code length, code weight, and number of users, the probability characteristic function of interference at the output of a correlator can be calculated as

$$\Phi_{\text{MA}}^{\text{OOC}}(z) = \left[\alpha' + \frac{\beta'}{2} \left[\exp(-m_r(1-z)) + \exp(-m_r(1-z^{-1})) \right] \right]^{N-1} \quad (39)$$

where $\beta' = w^2/F$ and $\alpha' = 1 - w^2/F$. Therefore, the multiuser interference variance for an OOC ($\lambda = 1$) system is

$$\sigma_{\text{OOC}}^2 = \left. \frac{\partial^2 \Phi_{\text{MA}}^{\text{OOC}}(z)}{\partial z^2} \right|_{z=1} = (N-1)w^2 m_r (1 + m_r) / F. \quad (40)$$

As can be seen, although OOC ($\lambda = 1$) codes are designed to have the minimum interference, they have the same multiuser interference variance as FTH patterns or generalized OOC. This indicates the reasons behind the close performance of FTH and OOC ($\lambda = 1$) systems as it was observed in Fig. 8.

The multiple-access performance of FTH patterns for several receiver structures can be also compared from Fig. 8. The correlation receiver with or without a hard limiter has a better performance than an (ordinary) chip-level detector for low mean received photoelectron counts per pulse. However, the chip-level detector is superior to the correlation for higher mean received photoelectron counts per pulse and reaches the optimum receiver performance for high powers. As can be predicted, the chip-level detector with optimum comparator threshold and the correlation receiver with an optical or electrical hard limiter are superior to an ordinary chip-level detector for low mean received photoelectron counts per pulse, however, they all tend to the optimum receiver performance as the received average power is increased. The chip-level detector with optimum comparator threshold performs a little worse than the correlation receiver for very low mean received photoelectron counts per pulse, but it performs considerably better than the simple correlation receiver for higher received average powers. There exist

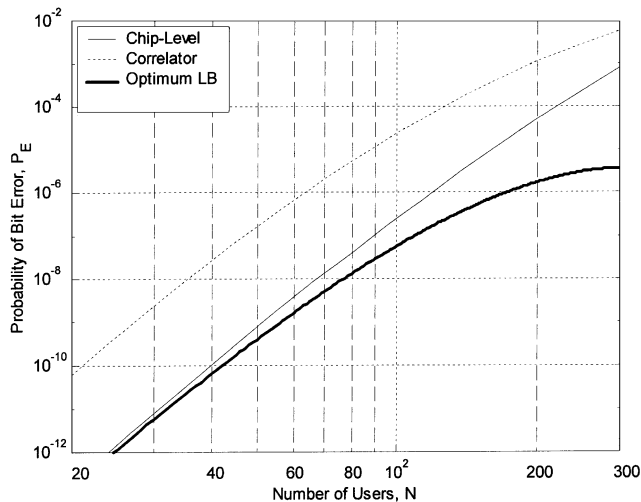


Fig. 9. Probability of bit error versus the number of users for various receiver structures with an ideal photodetector on a FTH system with $F = 2000$ and $w = 9$. Note that with an ideal photodetector, the chip-level detector with optimum comparator threshold and correlation receiver with a hard limiter are the same as a chip-level detector.

some breaks in the performance curve of the chip-level detector with optimum comparator threshold. These breaks correspond to the points in which the comparator switches its threshold to a higher level in order to achieve the minimum BER for higher mean received photoelectron counts per pulse. As can be observed, correlation with an electrical hard limiter is superior to all other suggested receivers for all ranges of received power. Moreover, this receiver reaches the optimum receiver performance for a mean received photoelectron count of ten, which is a factor of three, less than the other considered receivers.

Fig. 9 presents the probability of bit error versus the number of users for various receivers assuming an ideal photodetector. We recall that the performance of the chip-level detector with optimum comparator threshold and correlation with an optical or electrical hard limiter is the same as the chip-level detector with an ideal photodetector. The BER of the chip-level detector (or correlation receiver with a hard limiter) is a factor of 10 to 100 less than the correlation receiver in the same conditions, and is very close to the lower bound on the BER of the optimum receiver for a low or medium number of users. However, the gap between the BER curves of the chip-level detector and the optimum receiver increases as the number of users increases, mainly because the proposed lower bound on probability of error of the optimum receiver is not very tight for high BERs (or equivalently, a high number of users).

In Fig. 10, the BER of the correlation receiver is plotted as a function of the number of users for several mean received photoelectron counts per pulse. The performance of this receiver is close to the performance of the ideal photodetector case for a mean received photoelectron count of 20 per pulse, and increasing power to achieve a better performance is not necessary and not desirable.

Fig. 11 illustrates the BER for a chip-level detector (solid lines) and a chip-level detector with optimum comparator threshold for several received photoelectron counts per pulse versus the number of users. θ is selected to be one in this figure,

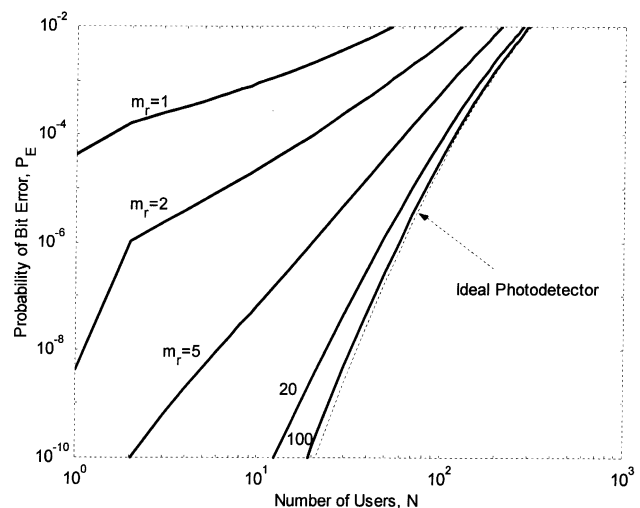


Fig. 10. BER of a correlation receiver on an FTH system with $F = 2000$ and $w = 9$ versus the number of users in various mean received photoelectron counts per pulse.

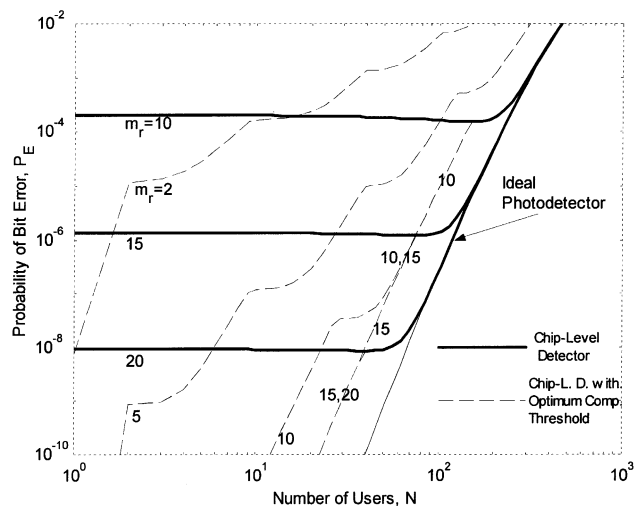


Fig. 11. BER of various receivers versus the number of users for an FTH system with $F = 2000$ and $w = 9$ in several mean received photoelectron counts per pulse.

i.e., the receiver decides that the signal is present in a slot if it detects only one photoelectron. As it can be seen in an ordinary chip-level detector, the BER is approximately constant for low number of users, since the dominant reason for error is the absence of power in at least one of the marked positions of the desired bit, which is determined mainly by the received mean photons per pulse and not the number of users. When the number of users is increased enough that the main reason of error would be due to the high received interference, the BER increases by increasing the number of users. On the other hand, a chip-level detector with optimum comparator threshold can achieve considerably lower BERs for a low number of users by selecting a lower comparator threshold. For a high number of users, both of the receiver performances tend to the performance of ideal photodetector case.

Fig. 12 shows the performance of the correlation receiver with a hard limiter. The performance of the correlation receiver with

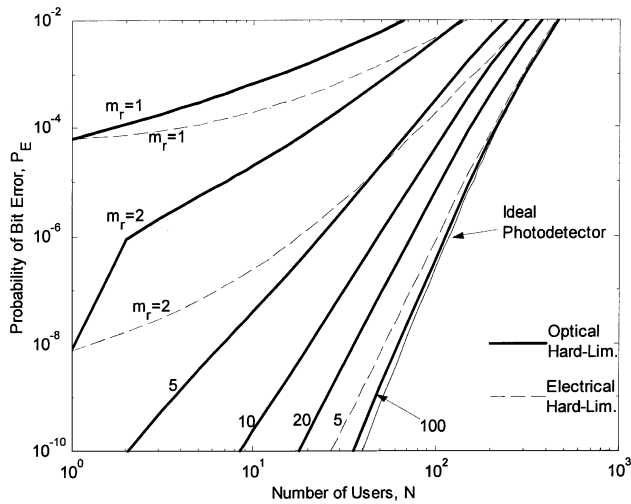


Fig. 12. BER of correlation receiver with an 1) optical hard-limiter and 2) electrical hard-limiter versus the number of users in various mean received photoelectron counts per pulse for a FTH system with $F = 2000$ and $w = 9$.

an electrical hard limiter is considerably better than the correlation receiver with an optical hard limiter in lower mean received photoelectron counts per pulse. Moreover, comparing Fig. 10 to Fig. 12, we see that the correlation receiver with any kind of hard limiter similar to a chip-level detector with optimum comparator threshold performs considerably better than the correlation receiver for all values of received power. On the other hand, a correlation receiver with an electrical hard limiter reaches the performance of the ideal photodetector case with much lower mean received photoelectron counts per pulse, e.g., with a mean photoelectron count of ten per pulse, the receiver performance is equal to the one of the ideal photodetector case. We recall that the performance of this receiver for the ideal photodetector case is equivalent to the performance of the optimum receiver also, that shows the overall superiority of this receiver to all other receivers considered in this paper.

V. CONCLUSION

In this paper, we proposed a new spreading technique for IM/DD FO-CDMA based on generalized OOCs. The main advantage of generalized OOCs is its high cardinality, i.e., the number of available codewords or simultaneous users in an optical network. We compared the multiple-access performance of this method to OOCs with autocorrelation and cross correlation bounded by one, for various receiver structures, including two newly proposed receiver structures, namely, chip-level detector with optimum comparator threshold and correlation receiver with an electrical hard limiter. The results indicate despite the less stringent constraints on the autocorrelation and cross-correlation bounds of generalized OOCs, its performance is close to the performance of the optimum codes, i.e., OOCs with $\lambda = 1$. The results also show that a chip-level detector with optimum comparator threshold presents considerably better performance in comparison with an ordinary chip-level detector for low received powers, while it inherits the desired features of an ordinary chip-level detector when compared to a simple correlation receiver for higher received powers. Furthermore, a corre-

lation receiver with an electrical hard limiter outperforms all the considered receivers in all received power ranges, and reaches the optimum receiver performance with much lower received power compared to a chip-level detector.

APPENDIX A

In this appendix, we obtain the decision rule for an optimum receiver considering multiuser interference and ideal photodetector (no shot noise) based on the number of received pulses in the first and the second slots of the marked chips following the methodology introduced in [9]. Let p_i and q_i , $1 \leq i \leq w$ be the number of pulses from other users that cause interference to the first and the second slot of chip number i , respectively. Further, let the vectors (p_1, p_2, \dots, p_w) and (q_1, q_2, \dots, q_w) be denoted by $\vec{p}^{(w)}$ and $\vec{q}^{(w)}$, respectively. Now consider N active users. There are $N - 1$ independent interfering users that interfere in each frame. Thus, the event $(P_1, Q_1) = (p_1, q_1)$, where P_1 and Q_1 are the random variables of the number of interfering pulses in the first and second slots of frame number 1, respectively, has the following trinomial distribution:

$$\begin{aligned} & \Pr\{(P_1, Q_1) = (p_1, q_1)\} \\ &= \binom{N-1}{p_1, q_1, N-1-p_1-q_1} (\beta/2)^{p_1} (\beta/2)^{q_1} \\ & \quad \cdot \alpha^{N-1-p_1-q_1} \\ &= \binom{N-1}{p_1, q_1, N-1-p_1-q_1} \left(\frac{\beta}{2\alpha}\right)^{p_1+q_1} \alpha^{N-1}. \quad (\text{A.1}) \end{aligned}$$

We assume that the events $(P_i, Q_i) = (p_i, q_i)$ and $(P_j, Q_j) = (p_j, q_j)$ for $i \neq j$ are independent. Thus

$$\begin{aligned} & \Pr\{\vec{P}^{(w)} = \vec{p}^{(w)}, \vec{Q}^{(w)} = \vec{q}^{(w)}\} \\ &= \prod_{i=1}^w \Pr\{(P_i, Q_i) = (p_i, q_i)\} \\ &= \prod_{i=1}^w \left[\binom{N-1}{p_i, q_i, N-1-p_i-q_i} \left(\frac{\beta}{2\alpha}\right)^{p_i+q_i} \alpha^{N-1} \right]. \quad (\text{A.2}) \end{aligned}$$

Assume $\vec{s}^{(w)} = (s_1, s_2, \dots, s_w)$ and $\vec{t}^{(w)} = (t_1, t_2, \dots, t_w)$ pulses are received in the first and the second slots of the marked chips, respectively. We denote by $\vec{S}^{(w)}$ and $\vec{T}^{(w)}$ the marked chips random variables, i.e., the vectors of the received pulses in the first and the second slots, respectively. In this case, the optimum receiver decides based on the following rule:

$$\begin{aligned} & \Pr\{1 \mid (\vec{S}^{(w)}, \vec{T}^{(w)}) = (\vec{s}^{(w)}, \vec{t}^{(w)})\} \\ & \stackrel{0}{\lesssim} \Pr\{0 \mid (\vec{S}^{(w)}, \vec{T}^{(w)}) = (\vec{s}^{(w)}, \vec{t}^{(w)})\}. \end{aligned}$$

Since $\Pr\{1\} = \Pr\{0\}$, the above is equal to

$$\begin{aligned} & \Pr\{(\vec{S}^{(w)}, \vec{T}^{(w)}) = (\vec{s}^{(w)}, \vec{t}^{(w)}) \mid 1\} \\ & \stackrel{0}{\lesssim} \Pr\{(\vec{S}^{(w)}, \vec{T}^{(w)}) = (\vec{s}^{(w)}, \vec{t}^{(w)}) \mid 0\}. \end{aligned}$$

When a "1" is transmitted, we have $\vec{S}^{(w)} = \vec{P}^{(w)}$ and $\vec{T}^{(w)} = \vec{Q}^{(w)} + \underbrace{(1, 1, \dots, 1)}_{w \text{ times}}$, and when a "0" is trans-

mitted, $\vec{S}^{(w)} = \vec{P}^{(w)} + \vec{I}^{(w)}$ and $\vec{T}^{(w)} = \vec{Q}^{(w)}$. Consequently, the optimum receiver is equivalent to

$$\begin{aligned} & \Pr\{(\vec{P}^{(w)}, \vec{Q}^{(w)} + \vec{I}^{(w)}) = (\vec{s}^{(w)}, \vec{t}^{(w)})\} \\ & \stackrel{0}{\leq} \Pr\{(\vec{P}^{(w)} + \vec{I}^{(w)}, \vec{Q}^{(w)}) = (\vec{s}^{(w)}, \vec{t}^{(w)})\} \\ & \equiv \Pr\{(\vec{P}^{(w)}, \vec{Q}^{(w)}) = (\vec{s}^{(w)}, \vec{t}^{(w)} - \vec{I}^{(w)})\} \\ & \stackrel{0}{\leq} \Pr\{(\vec{P}^{(w)}, \vec{Q}^{(w)}) = (\vec{s}^{(w)} - \vec{I}^{(w)}, \vec{t}^{(w)})\} \end{aligned}$$

or

$$\begin{aligned} & \prod_{i=1}^w \left[\binom{N-1}{s_i, t_i-1, N-s_i-t_i} \left(\frac{\beta}{2\alpha}\right)^{s_i+t_i-1} \alpha^{N-1} \right] \\ & \stackrel{0}{\leq} \prod_{i=1}^w \left[\binom{N-1}{s_i-1, t_i, N-s_i-t_i} \left(\frac{\beta}{2\alpha}\right)^{s_i+t_i-1} \alpha^{N-1} \right]. \end{aligned}$$

Simplifying the above equation, we obtain

$$\prod_{i=1}^w s_i \stackrel{0}{\leq} \prod_{i=1}^w t_i. \quad (\text{A.3})$$

APPENDIX B

To calculate the BER for the optimum receiver, we write

$$\begin{aligned} P_E &= P_{E|0} \\ &= \Pr\left\{\prod_{i=1}^w S_i < \prod_{i=1}^w T_i \mid 0\right\} + \frac{1}{2} \Pr\left\{\prod_{i=1}^w S_i = \prod_{i=1}^w T_i \mid 0\right\}. \end{aligned} \quad (\text{B.1})$$

A lower bound for the first part of the above equation can be written as

$$\begin{aligned} & \Pr\left\{\prod_{i=1}^w S_i < \prod_{i=1}^w T_i \mid 0\right\} \\ & \geq \Pr\left\{P_i = 0; \forall i, 1 \leq i \leq w \text{ and } \prod_{i=1}^w Q_i > 1\right\} \\ & = \Pr\{P_i = 0, Q_i \geq 1; \forall i, 1 \leq i \leq w\} \\ & \quad - \Pr\{P_i = 0, Q_i = 1; \forall i, 1 \leq i \leq w\} \\ & = (\Pr\{P_1 = 0, Q_1 \neq 0\})^w - (\Pr\{P_1 = 0, Q_1 = 1\})^w. \end{aligned}$$

On the other hand

$$\begin{aligned} & \Pr\{P_1 = 0, Q_1 \neq 0\} \\ & = \Pr\{P_1 = 0\} \Pr\{Q_1 \neq 0 | P_1 = 0\} \\ & = (1 - \beta/2)^{N-1} (1 - \Pr\{Q_1 = 0 | P_1 = 0\}) \\ & = (1 - \beta/2)^{N-1} \left(1 - \left(\frac{\alpha}{\alpha + \beta/2}\right)^{N-1}\right) \\ & = (1 - \beta/2)^{N-1} - (1 - \beta)^{N-1} \end{aligned}$$

and $\Pr\{P_1 = 0, Q_1 = 1\} = (1/2)(N-1)\beta(1-\beta)^{N-2}$ [see (A.2)]. Thus

$$\begin{aligned} & \Pr\left\{\prod_{i=1}^w S_i < \prod_{i=1}^w T_i \mid 0\right\} \geq [(1 - \beta/2)^{N-1} - (1 - \beta)^{N-1}]^w \\ & \quad - 2^{-w} [(N-1)\beta(1-\beta)^{N-2}]^w. \end{aligned} \quad (\text{B.2})$$

A lower bound for the second part of (B.1) can be calculated as

$$\begin{aligned} & \Pr\left\{\prod_{i=1}^w S_i = \prod_{i=1}^w T_i \mid 0\right\} \geq \Pr\{P_i = 0, Q_i = 1; 1 \leq i \leq w\} \\ & = (\Pr\{P_1 = 0, Q_1 = 1\})^w \\ & = 2^{-w} [(N-1)\beta(1-\beta)^{N-2}]^w. \end{aligned} \quad (\text{B.3})$$

Substituting (B.2) and (B.3) in (B.1), we have

$$\begin{aligned} P_E & \geq [(1 - \beta/2)^{N-1} - (1 - \beta)^{N-1}]^w \\ & \quad - 2^{-w-1} [(N-1)\beta(1-\beta)^{N-2}]^w. \end{aligned} \quad (\text{B.4})$$

ACKNOWLEDGMENT

The authors would like to thank Dr. M. Hakkak and Dr. M. Beik-Zadeh from Iran Telecom Research Center (ITRC) for support of this project.

REFERENCES

- [1] J. A. Salehi, "Code-division multiple-access techniques in optical fiber-optic networks—Part I: Fundamental principles," *IEEE Trans. Commun.*, vol. 37, pp. 824–833, Aug. 1989.
- [2] J. A. Salehi and C. A. Brackett, "Code-division multiple-access techniques in optical fiber-optic networks—Part II: System performance analysis," *IEEE Trans. Commun.*, vol. 37, pp. 834–842, Aug. 1989.
- [3] M. Azizoglu, J. A. Salehi, and T. Li, "Optical CDMA via temporal codes," *IEEE Trans. Commun.*, vol. 40, pp. 1162–1170, July 1992.
- [4] S. Zahedi and J. A. Salehi, "Analytical comparison of various fiber-optic CDMA receiver structures," *J. Lightwave Technol.*, vol. 18, pp. 1718–1727, Dec. 2000.
- [5] F. R. K. Chung, J. A. Salehi, and V. K. Wei, "Optical orthogonal codes: Design, analysis, and applications," *IEEE Trans. Inform. Theory*, vol. 35, pp. 595–604, May 1989.
- [6] R. A. Scholtz, "Multiple access with time-hopping impulse modulation," in *Proc. MILCOM'93*, Oct. 1993, pp. 447–450.
- [7] M. Z. Win, "Ultrawide-bandwidth spread-spectrum techniques for wireless multiple-access communications," Ph.D. dissertation, Univ. Southern Calif., Los Angeles, CA, 1998.
- [8] A. R. Forouzan, M. Nasiri-Kenari, and J. A. Salehi, "Performance analysis of time-hopping spread-spectrum multiple access systems: Uncoded and coded schemes," *IEEE Trans. Wireless Commun.*, vol. 1, pp. 671–681, Oct. 2002.
- [9] H. M. H. Shalaby, "Chip-level detection in optical code-division multiple-access," *J. Lightwave Technol.*, vol. 16, pp. 1077–1087, June 1998.
- [10] T. W. F. Chang and E. H. Sargent, "Optical CDMA using 2-D codes: The optimal single-user detector," *IEEE Commun. Lett.*, vol. 5, pp. 169–171, Apr. 2001.
- [11] C. W. Helstrom, "Approximate evaluation of detection probabilities in radar and optical communications," *IEEE Trans. Aerosp. Electron. Syst.*, vol. AES-14, pp. 630–340, July 1978.



Amir R. Forouzan was born on June 17, 1976, in Naein, Iran. He received the B.S. and M.S. degrees from the Sharif University of Technology (SUT), Tehran, Iran, in 1998 and 2000, respectively.

He is currently with the Department of Electrical and Computer Engineering, University of Tehran, Tehran, Iran. From 1999 to June, 2001, he was with the technical staff of Advanced CDMA Research Laboratory, Iran Telecom Research Center (ITRC), Tehran, Iran, and since July 2001, he has been with the Mobile Communications Division, ITRC. His

research interests include ultrawideband radio, radio and optical CDMA, and error-control coding.

Mr. Forouzan is a recipient of the Gold Medal of the Iranian Olympiad in Informatics.



Jawad A. Salehi (S'80–M'84) received the B.S. degree in electrical engineering from the University of California, Irvine, in 1979, and the M.S. and Ph.D. degrees from the University of Southern California (USC), Los Angeles, in 1980 and 1984, respectively.

From 1981 to 1984, he was a full-time Research Assistant at the Communication Science Institute, USC, engaged in research in spread-spectrum systems. From 1984 to 1993, he was a Member of Technical Staff with the Applied Research Area, Bell Communication Research (Bellcore), Morristown,

NJ. From February to May 1990, he was a Visiting Research Scientist with the Laboratory for Information and Decision Systems, Massachusetts Institute of Technology, Cambridge, where he conducted research on optical multiaccess networks. Currently, he is an Associate Professor with the Electrical Engineering Department, Sharif University of Technology, Tehran, Iran. From fall 1999 to fall 2001, he was the Head of the Mobile Communications Division and a Co-Director of the Advanced Communication Science Research Laboratory, Iran Telecommunication Research Center, Tehran, Iran. His current research interests are in optical multiaccess networks (CDMA), applications of EDFA in optical systems, and optical orthogonal codes. His work on optical CDMA systems has resulted in ten U.S. patents.

Dr. Salehi is a recipient of Bellcore's Award of Excellence. As a member of the organizational committee, he assisted in organizing the first and second IEEE Conferences on Neural Information. He currently serves as Editor for Optical CDMA for the IEEE TRANSACTIONS ON COMMUNICATIONS.

Masoumeh Nasiri-Kenari (S'92–M'93) received the B.S. and M.S. degrees in electrical engineering from the Isfahan University of Technology, Isfahan, Iran, in 1986 and 1987, respectively, and the Ph.D. degree in electrical engineering from the University of Utah, Salt Lake City, in 1993.

From 1987 to 1988, she was a Technical Instructor and Research Assistant at Isfahan University of Technology. Since 1994, she has been with the Department of Electrical Engineering, Sharif University of Technology, Tehran, Iran, where she is now an Associate Professor. She was a Co-Director of the Advanced CDMA Laboratory, Iran Telecom Research Center (ITRC), Tehran, Iran, in 1999–2001. Her research interests are in radio and optical communications and error-control coding.